

# Potentials of Heat Superimposed Rotary Friction Welding for Steel-Aluminium Joints

PIWEK, Armin<sup>1,a\*</sup>, PEDDINGHAUS, Julius<sup>1,b</sup>, UHE Johanna<sup>1,c</sup>,  
BRUNOTTE Kai<sup>1,d</sup> and BEHRENS Bernd-Arno<sup>1,e</sup>

<sup>1</sup>Institute of Forming Technology and Machines, Leibniz University Hannover, An der Universität 2,  
30823 Garbsen

<sup>a\*</sup>piwek@ifum.uni-hannover.de, <sup>b</sup>peddinghaus@ifum.uni-hannover.de,  
<sup>c</sup>uhe@ifum.uni-hannover.de, <sup>d</sup>brunotte@ifum.uni-hannover.de, <sup>e</sup>behrens@ifum.uni-hannover.de  
(\*corresponding author)

**Keywords:** Joining, Hybrid Materials, Heat Superimposition, Lightweight.

**Abstract.** Hybrid joints made of steel and aluminium alloy produced by rotary friction welding enable load-adapted lightweight components. However, a major challenge is the inhomogeneous radial temperature distribution caused by different relative velocities between the specimen centre and edge during rotation. This effect leads to local insufficient bonding and reduces the overall joint strength, especially in the centre, where low relative rotation speeds occur. Previous studies mainly addressed preheating before the friction phase, whereas superimposed heating during the upsetting phase has not been investigated so far. To achieve temperature equalisation along the cross-section during rotary friction welding, a modified KUKA Genius plus machine equipped with joule heating was used to introduce an electric current during the upsetting phase. Experiments were conducted on EN AW-6082 (AA-6082) joined to 20MnCr5 (AISI 5120H). A three-step variation of current intensity (10, 24 and 36 A/mm<sup>2</sup>), alongside a reference without current, was investigated. Temperatures were monitored using type K thermocouples, confirming temperature equalisation. Mechanical performance was assessed by uniaxial tensile tests, while hardness measurements and metallographic analyses characterised the influence of superimposed heating on the interfacial microstructure. Joint strength improves up to 17% with increasing current, even under otherwise unsuitable welding parameters that would normally result in insufficient bond strength. This improvement is linked to a uniform temperature distribution and enhanced material flow, resulting in a defect-free specimen centre.

## 1. Introduction

Increasing demands for energy-efficient and resource-conserving structures drive the development of hybrid lightweight components that combine high specific strength with reduced mass. Material systems such as steel-aluminium pairs offer substantial potential for functional integration and weight reduction, making them attractive for industrial applications ranging from automotive structures to production technology [1, 2].

Reliable and microstructurally controlled joining processes are essential, yet conventional fusion-based techniques frequently suffer from brittle intermetallic compound formation and inadequate suitability for dissimilar material pairings. Solid-state processes, particularly rotary friction welding (RFW), therefore offer a promising alternative due to lower heat input. Nevertheless, a major limitation arises from the inherent radial temperature gradient due to the increasing tangential velocity along the radius. With a maximum at the outer radius and a minimum of zero at the centre, uneven frictional heat generation develops on the welding surfaces. Consequently, different plastic strains and thus grain sizes occur along the radius in the subsequent upsetting phase, which can impair the homogeneity and strength of the joint [3, 4, 5]. To ensure sufficient temperatures and material flow, an increase in friction time and friction pressure is required. Efforts to mitigate radial temperature gradient have so far focused mainly before, after or in the friction phase, e. g., by adjusting process parameters [2, 6] or preheating the components [7, 8, 9]. The required thermal energy is provided by

an external heat input rather than by frictional heating alone. This approach drastically reduces the necessary upsetting force and friction time, resulting in minimal flash formation, reduced machine dimensions and smaller heat-affected zones compared to conventional friction welding [10, 11].

In addition to the ongoing development of methods aimed at achieving more homogeneous heat distribution, it appears promising to shift the research focus more strongly towards in-process concepts rather than purely pre- or post-weld treatments. Such strategies offer potential to meet both technological and economic requirements in industrial applications. Therefore, the present study provides the first systematic investigation of current assisted heating during the upsetting phase in RFW for the material pairing 20MnCr5 and EN AW-6082. The objective is to determine how an additional joule heating affects radial temperature equalisation, interfacial microstructure, specimen shortening and the tensile strength of the bond. The findings aim to deepen the understanding of thermomechanical interactions within the process and to identify industrially relevant potentials for more robust and functionally optimised hybrid lightweight joints in regards of material utilisation, mechanical load requirements, and overall process controllability.

## 2. State of the Art

### 2.1 Temperature Distribution in Rotary Friction Welding

RFW is a solid-state joining process in which two components are brought into axial contact, while one workpiece undergoes relative motion so that frictional heat is generated and the material at the interface becomes locally plasticised. Without the formation of a melt layer, the joining region is deformed and recrystallised, while the subsequent upsetting phase expels oxides as well as contaminants into the characteristic flash and establishes a sound metallurgical bond [5, 12]. Numerous studies confirm the suitability of RFW for both similar and dissimilar metallic combinations, as the short thermal cycles limit the growth of brittle intermetallic compounds and enable the formation of refined interface microstructures [1, 13]. Detailed microstructural analyses further indicate dynamically recrystallised grains and strong gradients in deformation and phase evolution within the thermo-mechanically affected zone [5]. However, the process also entails inherent challenges. Insufficient or uneven temperature development can hinder optimal plasticisation and promote the formation of critical intermetallic layers in dissimilar joints, particularly in aluminium-steel systems [1, 13]. These thermal limitations are a central motivation for recent studies exploring the use of additional external heating to homogenise the thermal boundary conditions and improve process stability and dissimilar joint performance.

A homogeneous and well-controlled temperature field is essential in RFW, since spatial thermal gradients govern local softening, interfacial shear conditions and the formation and growth of reaction layers. Several studies have demonstrated an inherent radially non-uniform thermo-mechanical field in RFW, as frictional heat generation increases with radius due to the linear rise in relative velocity. Experimental work by ALVES ET AL. on aluminium-steel confirmed the strong sensitivity of the joint to such temperature gradients, revealing incomplete plasticisation and reduced strength under insufficient heat input, while excessive thermal exposure promotes pronounced softening and material displacement [14]. Extending these findings, MISHRA ET AL. identified radial temperature gradients as a key factor driving radially heterogeneous plastic flow and interfacial deformation, particularly promoting weak bonding or defect formation in the joint centre [15]. In a similar study, MA ET AL. observed a reduction in strength for RFW joints between stainless steel X5CrNi18-10 and aluminium EN AW-2014 under both insufficient and excessive heat input. Insufficient thermal activation limited interfacial bonding, whereas excessive heat input promoted uneven and excessive growth of intermetallic compounds (IMC). Conclusively, only a moderate and radially balanced temperature field enabled the formation of a thin, continuous reaction layer and thus ensures a globally reliable joint [5]. Based on the presented studies, the aim is therefore to align the inhomogeneous heat distribution occurring in RFW with the more uniform temperature distributions prevailing in linear or orbital friction welding, since these processes yield a significantly more homogeneous heat input [4, 16]. This could not only promote the formation of more uniform

microstructural zones, but also contribute to improved and more consistent stress states in the upsetting phase, which would again increase joint strength.

## 2.2 Additional Heating in Rotary Friction Welding

Various approaches are currently being investigated in which the process is supplemented by an additional heat source. Many current studies focus on preheating one or both joining partners to ensure a more uniform temperature distribution in the joining zone. Within this context, DAHLAN ET AL. examined the effect of targeted preheating in combination with varying friction times on the joint strength of RFW between stainless steel X5CrNi18-10 and pure zinc semi-finished products. The steel component was heated to different target temperatures to reduce the effective friction time. Based on tensile tests, an increase in strength with a moderate preheating temperature of 100 °C could be observed. However, increasing the preheating temperature beyond this moderate level led to a reduction in tensile strength, which was attributed to increased enrichment of Fe, Cr, O, and C elements in the joining interface [17]. A similar conclusion was drawn by HAIBIN ET AL., who analysed preheating of the H59 brass component during RFW with EN AW-1100 aluminium to improve plastic deformation on the brass side while simultaneously controlling the formation of IMC. For this purpose, the brass part was heated to two different preheating temperatures by inductive heating immediately before welding. The highest joint strength was obtained at a temperature of 327 °C, which was attributed to the formation of a uniform, thin IMC of 3 µm. In contrast, preheating to 600 °C resulted in an excessively thick IMC of 16 µm and promoted thermally induced cracking, significantly reducing joint strength [18]. Beyond inductive preheating, alternative heat input strategies have also been explored. MULLO ET AL. investigated RFW between C45E steel and EN AW-2017-T4 aluminium while applying laser-based preheating to the steel component. In this case, increasing laser power consistently correlated with higher tensile strength, demonstrating that locally applied and controllable heat sources can effectively enhance joint performance [7].

Closely related to these concepts, the so-called low-force friction welding process has been developed by Manufacturing Technology, Inc. in collaboration with Edison Welding Institute. In this case, targeted preheating of the joining partners primarily serves to significantly reduce the process forces required during welding. In addition to induction heating, resistance-based external heating sources have also been tested for this process [19]. Apart from reduced process forces, this approach offers further advantages, including smaller flash formation, the possibility of using more compact machines, increased material compatibility, and shorter cycle times due to reduced friction time [10, 11].

Analogous to the upsetting phase of RFW, LIM ET AL. investigated a solid-state joining process based on a combination of Joule heating and mechanical pressure. The applied pressure was selected to match the intersection of the temperature-dependent yield strengths of the two materials Ti-6Al-4V titanium alloy and SUS316L stainless steel. In this way, uniform plastic deformation of both joining partners along the entire joint line could be achieved. The experimental results demonstrate that this process produces a significantly more homogeneous temperature distribution in the joining area compared with RFW. Notably, the temperature at the centre of the joining zone was slightly higher, which was attributed to increased cooling by ambient air in the peripheral region [20].

The reviewed studies clearly demonstrate the potentials of supplementing solid state welding with additional heat input to adjust the thermo-mechanical conditions in the joining zone. Preheating has been shown to improve joint strength and reduce process forces if applied within a narrow thermal window. However, excessive or poorly controlled heat input may lead to detrimental effects such as excessive IMC growth, microstructural degradation, or thermally induced cracking. Moreover, conventional preheating approaches often act globally on one joining partner and remain decoupled from the actual heat generation during the friction and upsetting phases. Therefore, the present work investigates a current-assisted RFW approach, in which additional heat is introduced directly into the joining zone by joule heating during upsetting. The objective is to perform a combined microstructural and mechanical evaluation of steel–aluminium joints, focusing on how different levels of electrical current modify the local thermo-mechanical conditions, interfacial microstructure, deformation behaviour, and resulting joint strength.

### 3. Materials and Methods

For the investigation, the case-hardening steel 20MnCr5 (AISI 5120H/1.7147) in the soft-annealed condition (hardness 180 HV1) as well as the heat-treatable aluminium alloy EN AW-6082 (AA-6082) in the T6 condition (hardness 100 HV1) were used. The chemical composition was measured by spark emission spectroscopy and is shown in **Tab. 1**.

**Table 1.** Chemical composition (mean value of 5)

	Si	Mn	Mg	C	Cr	Fe	Al
EN AW-6082	1.08	0.45	0.83	-	0.02	0.40	96.95
20MnCr5	0.24	1.29	-	0.17	1.07	97.04	0.02

The two materials were joined as cylindrical rods with a diameter  $D = 40$  mm and a length  $l = 100$  mm by means of RFW on a KUKA Genius Plus system (see **Fig. 1 a**). The friction welding setup includes a conductive heating unit consisting of copper conductors integrated into the clamping systems. During the upsetting phase, the specimens can be heated by a constant electric DC heating current based on the principle of resistance heating once the components are in contact. When the current is applied, the joining zone is additionally heated by the contact resistance at the faying surfaces of the semi-finished parts, in addition to the frictional heat introduced beforehand (see **Fig. 1 b**).

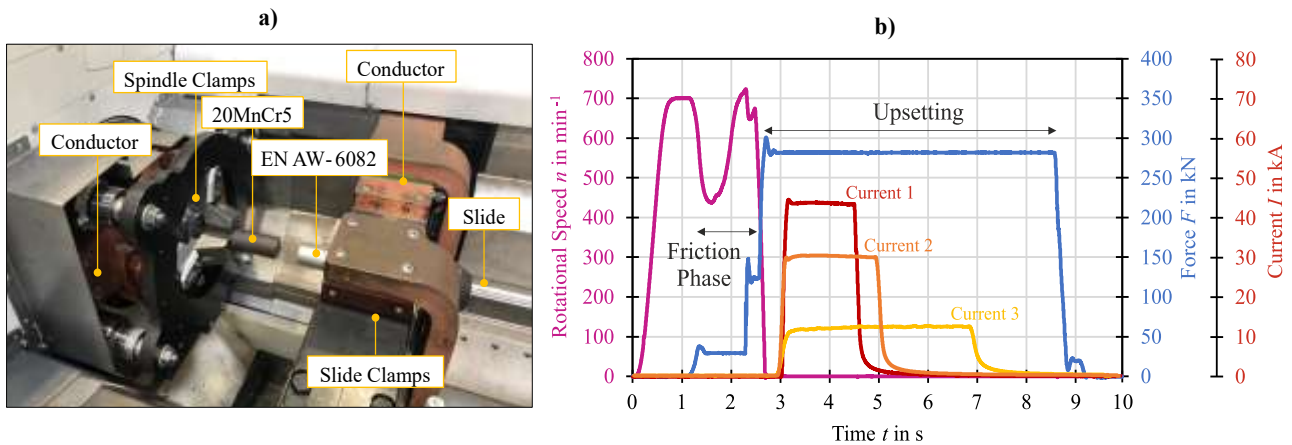


**Fig. 1. a)** Experimental setup of RFW with and without additional heating, **b)** exemplary RFW process with different current densities ( $n = 700 \text{ min}^{-1}$ ,  $p_F = 100 \text{ MPa}$ ,  $t_F = 0.2 \text{ s}$ ,  $p_U = 225 \text{ MPa}$ ).

At the beginning of the process, the clamped steel part is accelerated to a rotational speed of  $n = 700 \text{ min}^{-1}$ . In the beginning of the friction phase, the specimens are brought into contact for 1 s with an axial force of 35 kN. This is followed by the initial friction phase at a pressure of 100 MPa, during which the heat required for the process is generated. After the friction time ( $t_F$ ), the upsetting phase follows, in which an increased pressure ( $p_U$ ) is applied. Different current densities are set at the beginning of the upsetting phase and are varied between  $0 \text{ A/mm}^2$ ,  $10 \text{ A/mm}^2 \times 4 \text{ s}$ ,  $24 \text{ A/mm}^2 \times 2 \text{ s}$  and  $36 \text{ A/mm}^2 \times 1.5 \text{ s}$  for different friction times (0.1 s; 0.2 s) and upsetting pressures (150 MPa or 225 MPa). The electric current was applied exclusively during the upsetting phase, as this is the stage at which full interfacial contact is established under high axial pressure and relative motion has ceased. Under these conditions, resistance heating can be introduced in a controlled and localised manner directly at the joining interface. Applying current earlier would interfere with frictional heat generation and could promote premature softening of the aluminium alloy, leading to unstable process conditions and increased flash formation.

The experiments were carried out using a full factorial experimental design with twelve parameter sets using specimen shortening and tensile strength as a response variable. Uniaxial tensile testing was conducted to determine the bond strength using a universal testing machine of the AllroundLine Z250 type (ZwickRoell). The specimen geometry corresponds to a round tensile test specimen designed in accordance with DIN EN ISO 6892-1, with a gauge diameter of 30 mm and a gauge length of 85 mm. The reduction of the diameter is necessary to ensure fracture within this testing

method at a maximum test force of 250 kN. The comparability between the specimen series is not limited due to the identical machining. Furthermore, to evaluate the radial temperature distribution, temperatures were measured at a representative current density of 24 A/mm<sup>2</sup> using type K thermocouples positioned in the centre axis and at the periphery, approximately 6 mm from the joining zone, enabling a direct comparison between the conventional and the current-assisted process. Furthermore, to assess the influence of the electric current on the resulting microstructure, the specimens were characterised by metallographic analysis using light optical microscopy and hardness measurements.

## 4. Results and Discussion

### 4.1 Temperature Distribution

The temperature profiles presented in **Fig. 2 a** indicate a significant modification of the thermal behaviour when applying electric current in the joining process. For identical RFW parameters, the application of a current density of 24 A/mm<sup>2</sup> increases the absolute temperature level, with peak temperatures of 200 °C reached shortly after the end of the friction phase ( $t \approx 4$  s), compared to 125–160 °C in the conventional process. The apparent time delay in the temperature development is caused by transient heat conduction from the joining interface to the measurement positions. Since the thermocouples are located 6 mm from the weld interface, the recorded temperature reflects the thermal response of the surrounding material rather than the instantaneous interface temperature. As a result, temperature maxima occur with a temporal offset after changes in heat generation, particularly at the transition from the friction to the upsetting phase.

Without current assistance, the temperature reaches its maximum at the beginning of the upsetting phase and subsequently decreases. The lower relative velocities in the central region lead to delayed heat generation and, consequently, to pronounced radial temperature gradients, which are expected to be even more severe directly at the weld interface. With the introduction of electric current, additional heating in the joining zone is generated, effectively reducing the temperature gradient between the centre and the edge area, see **Fig. 2 b**. While the conventional process exhibits a maximum temperature difference of 56 K between centre and periphery, this gradient is reduced to about 16 K when electric current is applied, indicating a substantially more homogeneous thermal field.

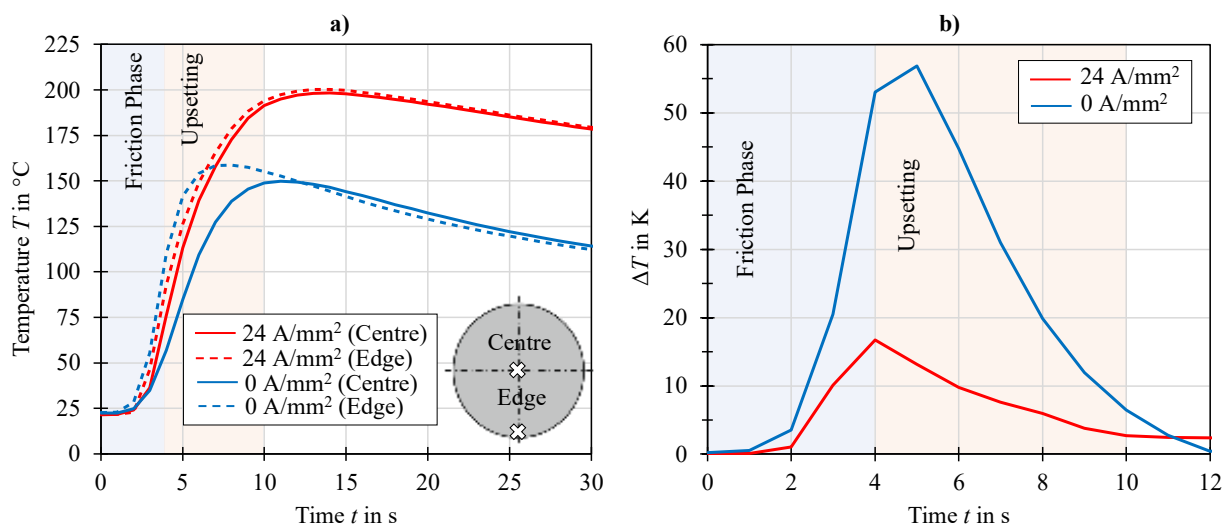


**Fig. 2.** Exemplary temperature curve, 6 mm distant to joining zone: **a)** measurements of the centre and edge area, **b)** temperature difference  $\Delta T$  between centre and edge ( $n = 700 \text{ min}^{-1}$ ,  $p_F = 100 \text{ MPa}$ ,  $t_F = 0.2 \text{ s}$ ,  $p_U = 225 \text{ MPa}$ ).

## 4.2 Flash Formation

Macroscopic cross-sections of joints between 20MnCr5 steel and EN AW-6082 aluminium produced at different current densities are shown in **Fig. 3**. In all cases, flash formation is predominantly observed on the aluminium side, while the steel component remains largely undeformed. The aluminium flash exhibits a characteristic curved and folded geometry, indicating pronounced plastic flow during the friction and upsetting phases. As a result of the upsetting pressure and the differing flow stresses depending on temperature, flash formation occurs, and the material displaced from the joining zone leads to a shortening of the semi-finished part, which should be avoided for both ecological and economic reasons.

With increasing current density, the flash becomes more pronounced. The observed flash formation is governed by the strongly temperature-dependent flow behaviour of the aluminium alloy. Compared to steel, EN AW-6082 exhibits significantly lower flow stresses, which decrease rapidly with increasing temperature [21]. While the steel component remains mainly undeformed due to its higher warm strength, the aluminium becomes highly plasticised in the joining zone and is displaced outward under the applied axial load. The application of electric current introduces additional resistance heating, increasing the local temperature beyond that generated by friction alone, as seen in **Fig. 3**.

Identical welding parameters were applied for all current densities. Therefore, the increased flash formation is primarily a consequence of the additional heat input provided by the electric current. Therefore, reduced friction times and lower axial forces may be applied while maintaining a sufficient plasticisation and flash formation. Overall, the superimposed heating expands the usable process window, allowing greater flexibility in parameter selection.

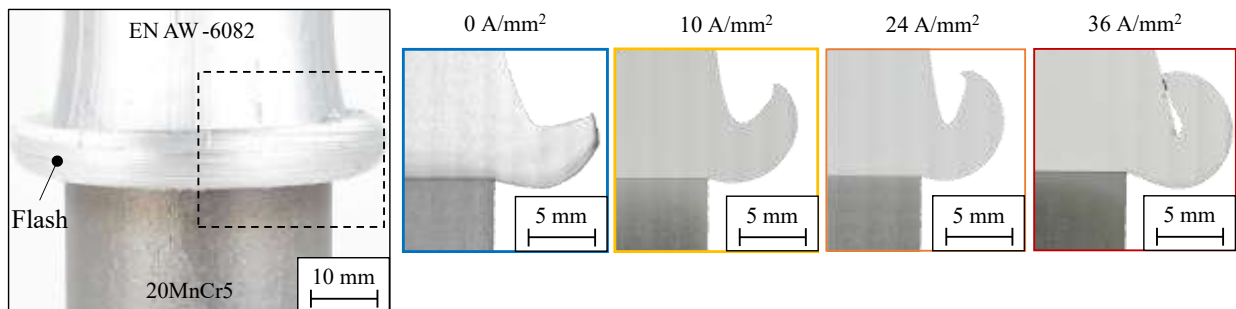


**Fig. 3.** Flash formation depending on current density, same RFW parameters ( $n = 700 \text{ min}^{-1}$ ,  $p_F = 100 \text{ MPa}$ ,  $t_F = 0,2 \text{ s}$ ,  $p_U = 225 \text{ MPa}$ ,  $t_U = 6 \text{ s}$ ).

## 4.3 Bond Strength and Shortening

To evaluate the effect of electric current on the bond strength, the RFW specimens were investigated by uniaxial tensile testing, and the resulting bond strength was correlated with the process-induced shortening, as shown in **Fig. 4 a** and **Fig. 4 b**. Overall, a beneficial influence of current assistance on the bond strength is evident.

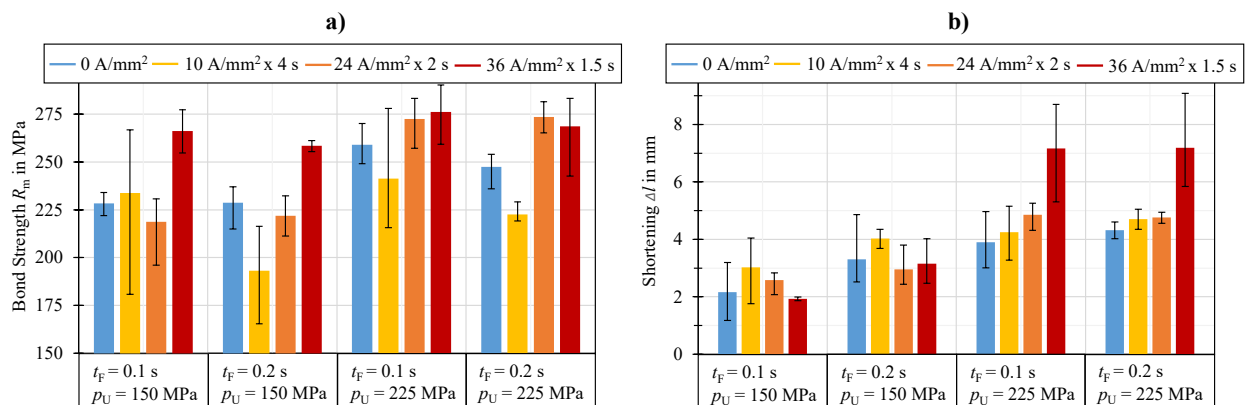


**Fig. 4. a)** Bond strength, **b)** specimen shortening, (3 measurements per parameter set)

Moderate to high current densities lead to a pronounced increase in bond strength. In particular, a density of  $24 \text{ A/mm}^2$  provides a favorable balance between high average strength (up to  $273 \text{ MPa}$ ) and similar material loss compared to  $0 \text{ A/mm}^2$ , making it advantageous from both a resource-efficiency and economic perspective. Although a higher current density of  $36 \text{ A/mm}^2$  enable high strengths of up to  $273 \text{ MPa}$  for short friction times, this advantage is diminished by the increased shortening if high upsetting pressures are present. However, at lower upsetting pressures of  $150 \text{ MPa}$ , current assistance ( $36 \text{ A/mm}^2$ ) allows a noticeable improvement up to  $17\%$  from  $228 \text{ MPa}$  to  $266 \text{ MPa}$  while maintaining a similar level of shortening compared to the reference. Therefore, the combination of reduced friction time and additional electrical heating effectively expands the usable process window, allowing mechanically less severe parameter combinations to achieve sufficient bonds. In contrast, at extended friction times of  $0.2 \text{ s}$ , a detrimental effect is observed for low current density ( $10 \text{ A/mm}^2$ ). This highlights that current assistance does not universally improve bond quality, but must be carefully matched with the friction time and upsetting pressure to achieve a beneficial thermal balance at a reduced material loss.

## 4.4 Metallography

### 4.4.1 Microstructural Characterisation

Pronounced differences in the microstructure are observed as a function of radial position and applied current density, as shown in **Fig. 5**.

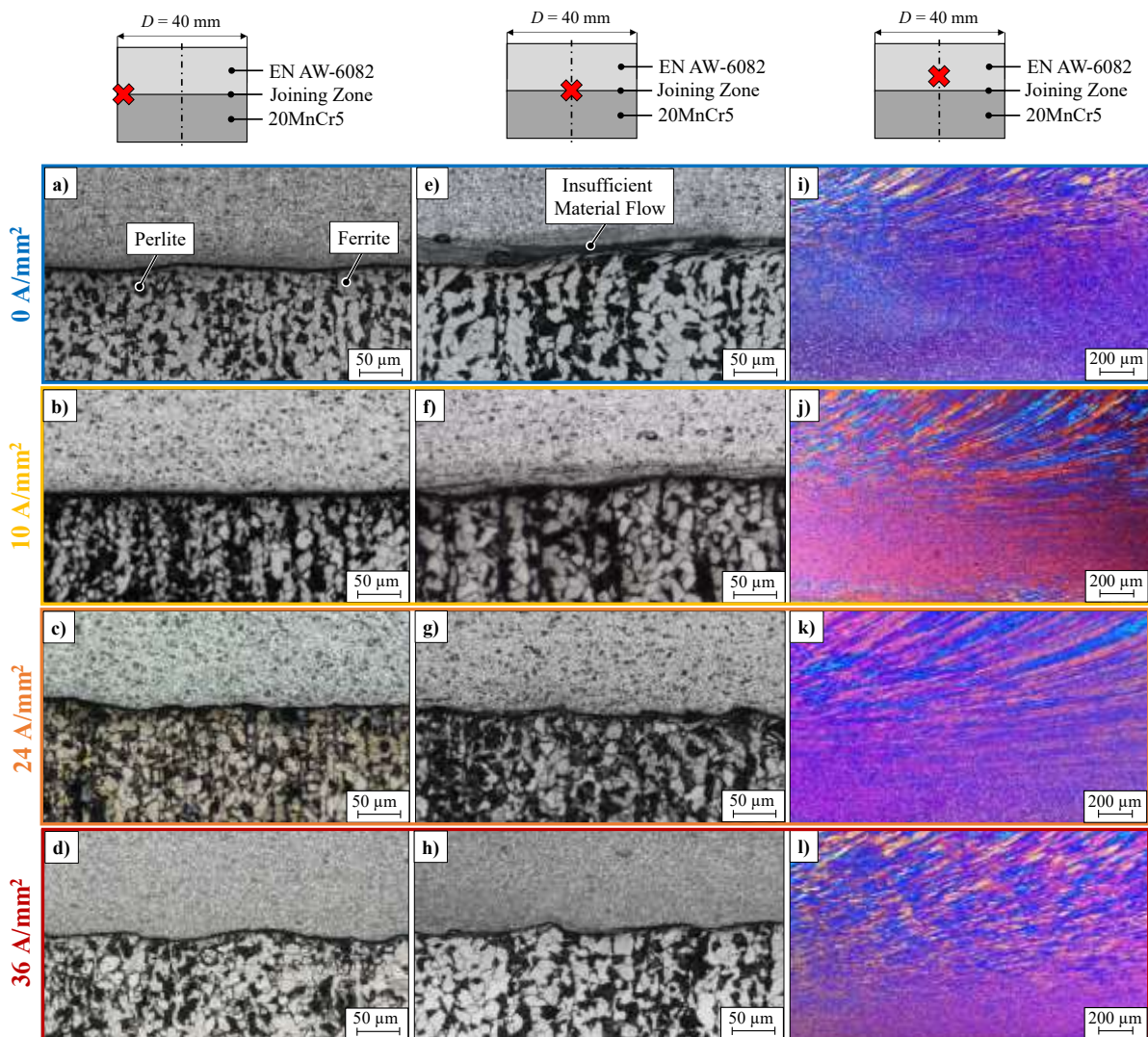


**Fig. 5.** Micrographs dependent on position and current density. Steel microstructure: **a) - d)** edge and **e) - h)** centre. **i) - l)** central microstructure in the aluminium ( $n = 700 \text{ min}^{-1}$ ,  $p_F = 100 \text{ MPa}$ ,  $t_F = 0,2 \text{ s}$ ,  $p_U = 225 \text{ MPa}$ ,  $t_U = 6 \text{ s}$ ).

In the edge region of the joint (**Fig. 5 a–d**), where frictional heat generation is highest, a continuous bonding interface is formed for all conditions. The steel exhibits a deformed ferritic–pearlitic microstructure adjacent to the joining line, with increasing waviness and plasticisation at higher current densities. In contrast, the centre of the joining zone (**Fig. 5 e–h**) indicate a strong dependence on current assistance. In the reference condition with 0 A/mm<sup>2</sup> (**Fig. 5 e**), the central interface is locally discontinuous, and regions of insufficient material flow are observed. The microstructural observations are characteristic of insufficient thermomechanical activation in the centre, where frictional heating is reduced, and align with central bonding defects reported in previous studies [1, 3, 15]. The steel microstructure appears strongly deformed but inhomogeneous, reflecting non-uniform local strain and temperature conditions rather than systematic grain coarsening or phase transformation effects. At a current density of 10 A/mm<sup>2</sup> (**Fig. 5 b, f**), the interfacial continuity is slightly improved compared to the reference condition. However, the centre still exhibits noticeable microstructural gradients, and localised flow deficiencies remain visible. The additional heat input at this current density is therefore insufficient to fully compensate for the reduced frictional heating in the centre.

At a current density of 24 A/mm<sup>2</sup> (**Fig. 5 c, g**), a continuous interface is formed across the entire joint width. The steel microstructure adjacent to the interface appears more uniformly plastified from edge to centre, and radial variations in interfacial morphology are reduced. This homogenisation indicates a more uniform thermal and deformation state, resulting from the combined action of mechanical friction and joule heating. The improved interfacial continuity is in good agreement with the enhanced bond strength observed for this condition.

At the highest current density of 36 A/mm<sup>2</sup> (**Fig. 5 d, h**), the interface remains continuous and uniform throughout the joint. Plastic deformation in the steel near the joining zone is present due to elevated temperatures and increased material flow. While no interfacial defects are observed, the microstructural appearance suggests an increased dominance of thermal effects, which correlates with the experimentally observed increase in axial shortening at higher upsetting forces.

The corresponding aluminium microstructures adjacent to the joining zone (**Fig. 5 i–l**) further support these findings. In the reference condition (**Fig. 5 i**), the aluminium exhibits oriented deformation bands, indicative of shear deformation under limited thermal softening. With increasing current density (**Fig. 5 j, k**), the deformation structures become progressively more diffuse, and orientation gradients are reduced. At 24 A/mm<sup>2</sup> and 36 A/mm<sup>2</sup>, the aluminium microstructure appears more homogeneous, reflecting enhanced thermal activation and a more uniform strain distribution near the interface.

Overall, based on the metallographic analysis, current-assisted RFW effectively reduces radial microstructural and interfacial gradients, particularly in the joint centre. Moderate current densities promote a homogeneous thermomechanical state in both joining partners, improving bonding conditions and hence suppressing central bonding defects. At excessively high current densities, microstructural homogenisation is maintained, but at the expense of increased thermal exposure, highlighting the importance of an optimised balance between electrical and mechanical heat input.

#### 4.4.2 Hardness Measurements

The steel-side hardness profiles remain on a comparable level for the reference condition (0 A/mm<sup>2</sup>) and current densities up to 24 A/mm<sup>2</sup>, with typical values of 175–200 HV in near the joining zone, see **Fig. 6**. At a current density of 36 A/mm<sup>2</sup>, a distinct hardness increase is observed, with local values reaching 200–220 HV. This increase cannot be explained by grain refinement, as metallographic analysis reveals local grain coarsening near the joining zone, see **Fig. 5**. Consequently, the classical Hall-Petch relationship is not the dominant strengthening mechanism in this case. Instead, the hardness increase is governed by deformation-induced strengthening, including elevated dislocation density and a strongly deformed ferrite–pearlite morphology resulting from intensified plastic flow during welding and upsetting. Such deformation-related effects are known to outweigh grain-size-related softening when recovery and recrystallisation remain incomplete [22].

On the aluminium side, a pronounced hardness minimum is observed near the joining zone for all conditions, with values decreasing to 75 HV, followed by a gradual recovery towards the base material. At higher current densities, this local softening becomes slightly less pronounced, reflecting increased thermal exposure and plastic deformation, which is consistent with the observed material flow and flash formation. During upsetting, the additional heat input leads to a pronounced reduction in the flow stress of aluminium, promoting intensified radial material flow both in the joint centre and edge area. Thermally softened aluminium is preferentially extruded outward during upsetting, forming an enlarged flash and removing highly heated material from the interface [1, 3, 15].

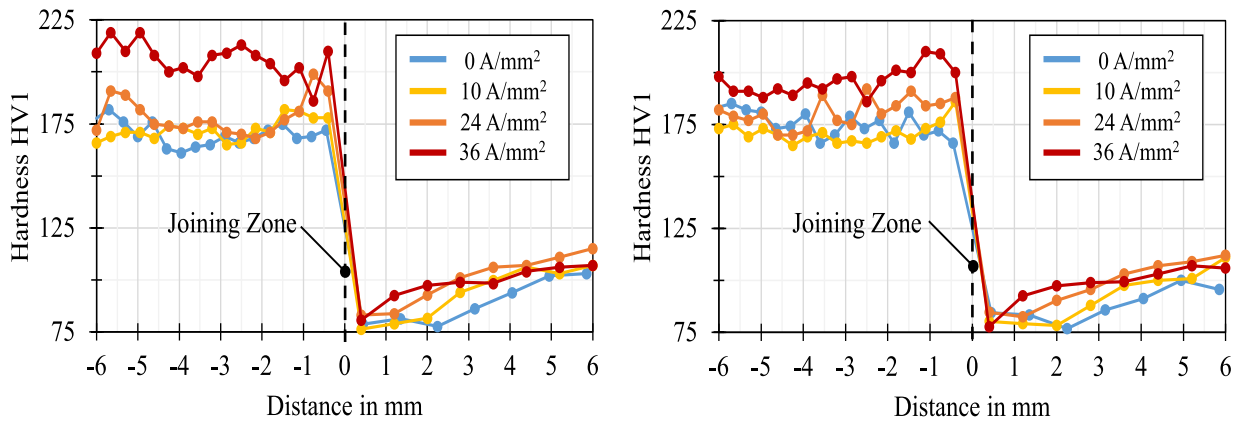


**Fig. 6.** Hardness measurements. **a)** Hardness in the centre, **b)** hardness 10 mm distant from the edge. ( $n = 700 \text{ min}^{-1}$ ,  $p_F = 100 \text{ MPa}$ ,  $t_F = 0,2 \text{ s}$ ,  $p_U = 225 \text{ MPa}$ ,  $t_U = 6 \text{ s}$ ).

## 5. Summary

The application of electric current leads to a homogenisation of the temperature distribution between the centre and the peripheral regions. With increasing current density, the bond strength further improves up to 17% compared to the reference condition. Moreover, the use of electric current reduces the axial force required during the upsetting phase to achieve a high-strength joint. This reduction in the upsetting force required potentially allows larger cross-sections to be joined without the need to increase the mechanical capacity of the machine. Although shortening increases with current application for identical process parameters, an appropriate adjustment of the process parameters allows a reduction in material loss and cycle time. As a result, parameter sets that would be unsuitable without current assistance can be potentially applied.

## 6. Outlook

For future work, local tensile tests at different radial positions are planned to assess the local joint quality along the radius in greater detail. In addition, the influence of current application on the radial distribution of intermetallic compounds will be investigated. A further outlook includes the welding of materials that are conventionally considered unsuitable due to mismatched thermal expansion behaviour, which otherwise prevents the formation of a sufficient joint. Finally, with regard to economic and environmental aspects, a comparative analysis of electrical energy consumption, process efficiency, and potential material savings is envisaged. Based on these factors, the associated CO<sub>2</sub>-emission reduction potential of the respective processes can be quantified.

## Acknowledgement

Funded by the Deutsche Forschungsgemeinschaft (DFG, German Research Foundation) – CRC 1153 subproject B03 – 252662854. The authors thank KUKA Deutschland GmbH for providing the conductive heating unit.

---

**References**

- [1] E. Taban, J.E. Gould, J.C. Lippold, Dissimilar friction welding of 6061-T6 aluminum and AISI 1018 steel: Properties and microstructural characterization, *Mater. Des.* 31 (2010) 2305–2311. <https://doi.org/10.1016/j.matdes.2009.12.010>
- [2] M. Ghari, A. Ghasemi, B. Kondori, Microstructural evolution and mechanical properties of dissimilar steel–aluminium rotary friction welded joints, *J. Mater. Process. Technol.* 213 (2013) 1691–1700. <https://doi.org/10.1016/j.jmatprotec.2013.03.018>
- [3] N. Gotawala, A. Shrivastava, Investigation of interface microstructure and mechanical properties of rotatory friction welded dissimilar aluminum–steel joints, *Mater. Sci. Eng. A* 825 (2021) 141900. <https://doi.org/10.1016/j.msea.2021.141900>
- [4] M. Maalekian, E. Kozeschnik, H.P. Brantner, H. Cerjak, Comparative analysis of heat generation in friction welding of steel bars, *Acta Mater.* 56 (2008) 2843–2855. <https://doi.org/10.1016/j.actamat.2008.02.016>
- [5] H. Ma, G. Qin, P. Geng, S. Wang, D. Zhang, Microstructural characterisation and corrosion behaviour of aluminium alloy/steel hybrid structure produced by friction welding, *J. Manuf. Process.* 61 (2021) 349–356. <https://doi.org/10.1016/j.jmapro.2020.11.014>
- [6] M. Winkler, C. Rößler, N. Harriehausen, S. Jüttner, D. Schmicker, F. Trommer, An energetic approach to the statistical analysis and optimization of friction welding processes applied to an aluminum–steel joint, *J. Adv. Joining Process.* 10 (2024) 100251. <https://doi.org/10.1016/j.jajp.2024.100251>
- [7] J.L. Mullo, J.A. Ramos-Grez, G.O. Barrionuevo, Effect of Laser Heat Treatment on the Mechanical Performance and Microstructural Evolution of AISI 1045 Steel–2017-T4 Aluminum Alloy Joints during Rotary Friction Welding, *J. Mater. Eng. Perform.* 30 (2021) 2617–2631. <https://doi.org/10.1007/s11665-021-05614-6>
- [8] G. L. Wang, J. L. Li, „Rotary friction welding on dissimilar metals of aluminum and brass by using pre-heating method“, *The International Journal of Advanced Manufacturing Technology*, 2018. <https://doi.org/10.1007/s00170-018-2572-y>
- [9] M.R. Kelly, S.R. Schmid, D.C. Adams, J. Fletcher, R. Heard, Experimental investigation of linear friction welding of AISI 1020 steel with pre-heating, *J. Manuf. Process.* 39 (2019) 26–39. <https://doi.org/10.1016/j.jmapro.2019.01.038>
- [10] P. Żurawski, Perspectives of the low force friction welding process, *Manuf. Technol.* 22 (2022) 633–643. <https://doi.org/10.21062/mft.2022.067>
- [11] P. Żurawski, Analysis of low force friction welding process in the industrial environment, *Int. J. Eng. Innov. Technol.* 11 (2022) 1–9. <https://doi.org/10.51456/IJEIT.2022.v11i07.001>
- [12] U. Dilthey, *Schweißtechnische Fertigungsverfahren 1: Schweiß- und Schneidtechnologien*, Springer-Verlag, Berlin / Heidelberg, 2006. <https://doi.org/10.1007/3-540-33154-9>
- [13] S. Herbst, H. J. Maier, F. Nürnberger, Strategies for the Heat Treatment of Steel-Aluminium Hybrid Components, *HTM J. Heat Treatm. Mat.* 73 (2018) 5, 268–282, <https://doi.org/10.3139/105.110368>
- [14] E.P. Alves, F.P. Neto, C.Y. An, E.C. da Silva, Experimental determination of temperature during rotary friction welding of AA1050 aluminum with AISI 304 stainless steel, *J. Aerosp. Technol. Manag.* 4 (2012) 61–67. <https://doi.org/10.5028/jatm.2012.04013211>
- [15] N. K. Mishra, A. K. Singh, S. K. Panda et al., Interfacial inhomogeneous plastic deformation during rotary friction welding of dissimilar materials, *J. Adv. Join. Process.* 10 (2024) 100245. <https://doi.org/10.1016/j.jajp.2024.100245>

- 
- [16] I. Martinek, H. Goldau, und F. Trommer, “Grundsatzuntersuchungen zum Orbitalreibschweißen des unlegierten Baustahls S355J2,” Innovationspreis Reibschweißen, 2010. [Online]. Available: [https://www.raiser.de/images/download/reibschweissen/innovationspreis/bewerber2011/frank\\_trommer.pdf](https://www.raiser.de/images/download/reibschweissen/innovationspreis/bewerber2011/frank_trommer.pdf)
- [17] H. Dahlan, A.K. Nasution, S.A. Zuhdi, M. Rusli, Study of the effect of friction time and preheating on the joint mechanical properties of friction welded SS316–pure Zn, *Appl. Sci.* 13 (2023) 988. <https://doi.org/10.3390/app13020988>
- [18] G. Haibin, X. Guifeng, L. Jingcheng, L. Hao, Rotary friction welding of pure aluminum to preheated brass, *Weld. World* 66 (2022) 2371–2376. <https://doi.org/10.1007/s40194-022-01367-5>
- [19] Z. Roelofs, J. E. Gould, Preliminary results on low force friction welds of dissimilar materials: Aluminum 6061 to 1020 steel tubes. In: *Low Force Friction Welding of Bimetallics*, Manufacturing Technology, Inc., 2020.
- [20] Y. Lim, Y. Morisada, H. Liu, und H. Fujii, “Ti-6Al-4V/SUS316L dissimilar joints with ultrahigh joint efficiency fabricated by a novel pressure-controlled joule heat forge welding method,” *Journal of Materials Processing Technology*, vol. 298, p. 117283, 2021, <https://doi.org/10.1016/j.jmatprotec.2021.117283>
- [21] F.J. Humphreys, M. Hatherly, *Recrystallization and Related Annealing Phenomena*, 2nd ed., Elsevier, Oxford, 2004. <https://doi.org/10.1016/B978-0-08-044164-1.X5000-2>
- [22] I. Schindler, P. Kawulok, V. Očenášek, et al. Flow Stress and Hot Deformation Activation Energy of 6082 Aluminium Alloy Influenced by Initial Structural State *Metals* 9 (2019) 1248. <https://doi.org/10.3390/met9121248>